Eur. J. Hortic. Sci. *89*(6) | ISSN 1611-4426 print, 1611-4434 online | https://doi.org/10.17660/eJHS.2024/032 | © ISHS 2024

Original article

Effects of cutting parameters on the ultimate shear stress and specific cutting energy of Canadian goldenrod stem

Ziyu Li[1], Guanqun Wang[1], Weidong Jia[1], Mingxiong Ou[1], Xiang Dong[1], Tie Zhang[2], Hong Chen[1] and Chenyang Wang[1]

[1] School of Agricultural Engineering, Jiangsu University, Zhenjiang, China
[2] Chinese Academy of Agricultural Mechanization Sciences Group Co., Ltd., Beijing, China

Summary

Due to the lack of weed-specific designs in weeding equipment, this article conducted cutting experiments on one type of weed: Canadian goldenrod. This study examined the influence of various cutting parameters on the process of cutting Canadian goldenrod stems to determine the optimal cutting parameters. A quasi-static cutting method was used to cut the stems. The results indicated that cutting speed, stem oblique angle, blade oblique angle, and stem diameter significantly affected the ultimate shear stress and specific cutting energy during the cutting process. The response surface method was employed to explore the optimal cutting parameters. In this experiment, the minimum combined values of ultimate shear stress and specific cutting energy were achieved when the cutting speed, stem oblique angle, blade oblique angle, and stem diameter were 30 mm s^{-1}, 20°, 0°, and 6 mm, respectively. When cutting close to the ground, the optimized cutting method reduced the ultimate shear stress and specific cutting energy by 52.68% and 55.22%, respectively, compared to ordinary cutting. These optimal cutting parameters can support the blade layout and output power design of a weeder or harvester.

Keywords
precision plant protection, quasi static cutting, response surface method, weed cutting, optimal cutting parameters, *Solidago canadensis*

Significance of this study

What is already known on this subject?

- Canadian goldenrod is a widely distributed and highly detrimental invasive plant. However, it also has medicinal properties. Currently, there are few researches about the physical characteristics of Canadian goldenrod stems.

What are the new findings?

- Cutting speed, stem angle, blade angle, and diameter significantly affect the cutting process of Canadian goldenrod stems. In quasi-static cutting, optimal conditions are achieved when these parameters are set at 30 mm s^{-1}, 20°, 0°, and 6 mm, respectively.

What is the expected impact on horticulture?

- This provides guidance for reducing the force and energy consumption when cutting Canadian goldenrod stems, whether through manual or mechanical methods, and also guides the design of targeted cutting blades.

Introduction

Canadian goldenrod (*Solidago canadensis*) is a perennial herb of the *Asteraceae* family that originated in North America (Wang et al., 2019). Canadian goldenrod is both a harmful plant that can cause ecological damage and an economic plant that can be used to prepare various materials (Leitner et al., 2012; Tu et al., 2023; Zhang and Wan, 2017). In China, it is a notorious invasive species with a wide invasion range, causing significant harm (Abhilasha et al., 2008; Ruyi et al., 2008; Zhao et al., 2015; Zhang and Wan, 2017; Hu et al., 2021). However, in Europe, Canadian goldenrod has been used for medical treatment for nearly 700 years (Suleymanova et al., 2020; Apati et al., 2003). *S. canadensis* in Canadian goldenrod has medicinal value as an antioxidant, bactericidal, and anti-inflammatory substance (Zhang and Wan, 2017). Additionally, Canadian goldenrod is a potential high-quality raw material for the preparation of activated carbon for high-performance supercapacitors (Tu et al., 2023). In order to harvest goldenrod and suppress its sexual reproduction, which is crucial for its proliferation (Dong et al., 2006), it is necessary to understand its cutting characteristics to avoid incomplete cuts and energy waste.

Cutting force and energy consumption are key factors in measuring cutting quality during the cutting process (Aydın and Arslan, 2018), where physical properties and cutting parameters are the main influencing factors. The physical properties of the material to be cut are considered plant characteristics, while the cutting parameters are working characteristics (Rabbani et al., 2015). Yunfeng et al. (2016) measured the elastic modulus of cucumbers at different positions to gain a deeper understanding of their cutting performance. Zhao et al. (2022) measured the contents of the rind and xylem of broccoli at different positions, as well as the elastic modulus, compressive elastic modulus, and bending modulus. These data form the basis of the mechanical model for broccoli.

When studying cutting parameters, cutting speed (Maughan et al., 2014), stem oblique angle, and blade oblique angle (Dange et al., 2011) should all be assessed. Ghahraei et al. (2008) conducted a sweet sorghum cutting test and found that the cutting force at a blade oblique angle of 30° was less than that at 45°; Hu et al. (2023) consider that cutting with blade oblique angle, which is sliding cutting, helps reduce cut-

ting resistance. Through experimentation, Wang et al. (2022) found that as the blade oblique angle increases from 0° to 60°, both the maximum cutting stress and the specific cutting energy decrease. Mathanker et al. (2015) indicated that when cutting sorghum stalks, the specific energy required for cutting increased with cutting speed. The stem oblique angle refers to the angle between the stem and the blade, while the blade oblique angle refers to the angle between the blade and the blade clamp. Since Canadian goldenrod usually grows vertically, the stem oblique angle and the blade oblique angle can jointly determine the general design of the cutting parts of the machine. Rabbani et al. (2015) indicated that the effective cutting coefficient increases with the cutting bevel angle. Song et al. (2022) showed that when the stem oblique angle increases from a negative value to 0, the ultimate shear stress and specific cutting energy both increase, while when the stem oblique angle increases from 0, both the ultimate shear stress and specific cutting energy decrease. Johnson et al. (2012) compared the cutting energy at three different blade oblique angles and found that when the blade oblique angle was between 0° and 60°, a larger blade oblique angle resulted in lower cutting energy. Du et al. (2015) used the factorial design method to determine the best cutting parameters for harvesting cabbage: a sliding angle of 40°, a cutting speed of 300 mm min^{-1}, and a cutting diameter of 35 mm. Vu et al. (2020) used response surface methodology to optimize the cutting of corn straw, and the optimized cutting force and energy consumption were reduced by 2.3 times and 4 times, respectively.



Figure 1. Cutting experimental device.

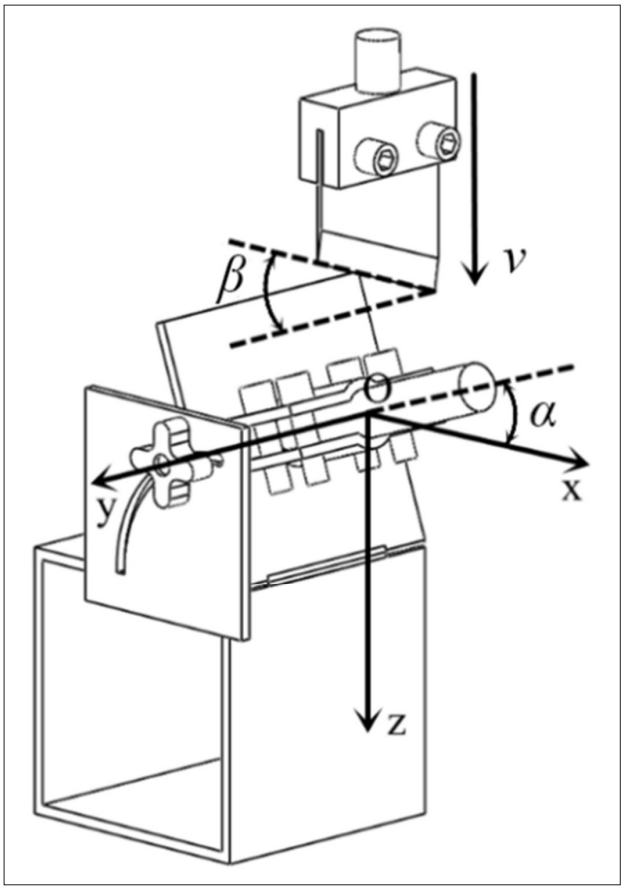


Figure 2. Relative position of the test equipment in the Cartesian coordinate system.

Due to the current lack of data supporting mowing operations, energy waste often occurs during mowing. The aim of this paper is to optimize the weeding method and mower design by exploring the physical properties of Canadian goldenrod stems and quantifying the optimal cutting parameters.

Materials and methods

Canadian goldenrod stem

The Canadian goldenrod stems used in this study were collected from the wilderness near Jiangsu University when the plants were about to bloom. The university is located in a subtropical monsoon climate. Canadian goldenrod, measuring 1.2 to 1.6 m in height, was randomly collected in October, prior to flowering. A saw was used to cut the stems close to the ground during collection. In total, 195 samples were obtained.

After collection, all cutting experiments were completed within 10 h to ensure that the physical properties of the samples did not change significantly. Following the cutting experiments, all samples were dried using a constant temperature blast dryer to measure their moisture content (ASABE Standards, 2008). The laboratory temperature was approximately 20°C, and the relative humidity was around 60%, which did not have a significant impact on the moisture content of the samples. The moisture content of the samples ranged between 44.12% and 57.03%.

Experimental system

Quasi-static cutting is a method of cutting at the slowest possible speed to obtain a more detailed cutting process. This method is commonly used to study the physical properties and cutting processes of samples (McRandal and McNulty, 1978). In these cutting experiments, a texture analyzer and the accompanying Exponent Stable Micro Systems software, which can record various parameters during cutting, were used. The stems were secured with an adjustable clamp, as shown in Figure 1. The texture analyzer recorded the cutting force-displacement curve. The blade used in the machine was a Stanley FatMax heavy-duty cutter. The stems were fixed at one end to simulate actual weeding conditions.

Table 1. Value and level of cutting factors.

Level	Cutting speed, v (mm s^{-1})	Stem oblique angle, α°	Blade oblique angle, β°	Diameter, D (mm)
-2	10	−20	0	6
-1	15	−10	10	7
0	20	0	20	8
1	25	10	30	9
2	30	20	40	10

The positions of the stem, blade, and clamp in the Cartesian coordinate system are defined as shown in Figure 2. The XOY plane is horizontal, and the z-axis is vertical. The origin O of the coordinates is on the centerline of the sample, which is also on the blade plane. The blade plane coincides with the XOZ plane, and the blade's moving direction is consistent with the positive direction of the z-axis. The stem oblique angle α is defined as the angle between the stem and the positive direction of the y-axis (Vu et al., 2020). The blade oblique angle β is defined as the angle between the blade edge and the negative direction of the x-axis. The distance between the YOZ plane and the clamping position is less than 2 mm. During the experiment, angles α and β were adjusted to change the relative positions of the stem and blade.

Data analysis

This article treats the cross-section of the stem as a circle, which is directly determined from its diameter. Based on the peak cutting force (F_{max}) and the area under the cutting force-displacement curve (A_c), both of which can be obtained using Exponent Stable Micro Systems software, two parameters used to evaluate the cutting process can be calculated: the maximum shear stress that the stem can withstand (ultimate shear stress, MPa) and the energy required per unit area during cutting (specific cutting energy, ×10^{-3} J mm^{-2}). These parameters are calculated using the following equation (Tang et al., 2022):

$$\tau = \frac{F_{max}}{A} \quad (1)$$

Where:
τ = ultimate shear stress (MPa);
F_{max} = the peak cutting force (N);
A = the sample cross-sectional area (mm^2).

Using Exponent Stable Micro Systems software, we can obtain the cutting force-displacement curve area A_c (mm s^{-1}):

$$A_c = \frac{1}{v}\int_0^s F ds \quad (2)$$

The specific cutting energy (×10^{-3} J mm^{-2}) can be obtained by equation(3):

$$E_{pur} = \frac{1}{A}\int_0^s F ds \quad (3)$$

Then, we can obtain a simple equation for the specific shear energy:

$$E_{pur} = \frac{v}{A} A_c \quad (4)$$

Where:
E_{pur} = specific cutting energy (×10^{-3} J mm^{-2});
A_c = cutting force-displacement curve area;
v = cutting speed (mm s^{-1}).

The cross-section of the Canadian goldenrod stem was considered a circle in the calculation.

Experimental design

The experiment consisted of two parts: a single-factor cutting experiment and a response surface cutting experiment. In the single-factor cutting experiment, the influence of each parameter on cutting was studied individually. After understanding the effects of different factors on cutting, a response surface cutting experiment was conducted using the central composite experimental design and Design Expert 11 (Stat-Ease). Response surface methodology is a mathematical tool commonly used to optimize operating conditions and derive variable equations (Engmann et al., 2014). Each experiment in both parts was repeated three times.

Since the Canadian goldenrod used in the study grew in the wild, its growth environment may have varied significantly, with inconsistent light, growth space, soil nutrition, and germination times. As a result, the physical properties of the stems could differ. To ensure accuracy despite these uncontrollable factors – including the mechanical and biological variability of the stems (Wu and Song, 2022) – when there was a large variation in results, the test was repeated 5 to 8 times, and outlier data were excluded. The values and levels of the cutting factors are listed in Table 1.

Results

Effects of cutting parameters on cutting Canadian goldenrod stem

Under the guidance of the single-factor experimental method (Wang et al., 2020), the effects of cutting parameters on cutting were analyzed one by one. When discussing one cutting parameter, the other parameters were fixed at level 0, as shown in Table 1. The results are presented in Figure 3.

Effects of interactive items on cutting of Canadian goldenrod stems

With the support of Design Expert 11 (Stat-Ease) and using the central composite design module, response surface analysis experiments were conducted with cutting speed (v), stem oblique angle (α), blade oblique angle (β), and diameter (D) as parameters, while ultimate shear stress and specific cutting energy were used as responses. Each parameter had 5 levels. The specific experimental results are shown in Table 2.

Table 3 shows the variance analysis of the results for ultimate shear stress and specific cutting energy. Both models are significant ($P < 0.0001$), and the lack-of-fit term is not significant ($P > 0.05$), indicating that both models are accurate and can be used for further prediction. Only four factors and their pairwise interactions were considered, as including more factors would reduce the feasibility of the model.

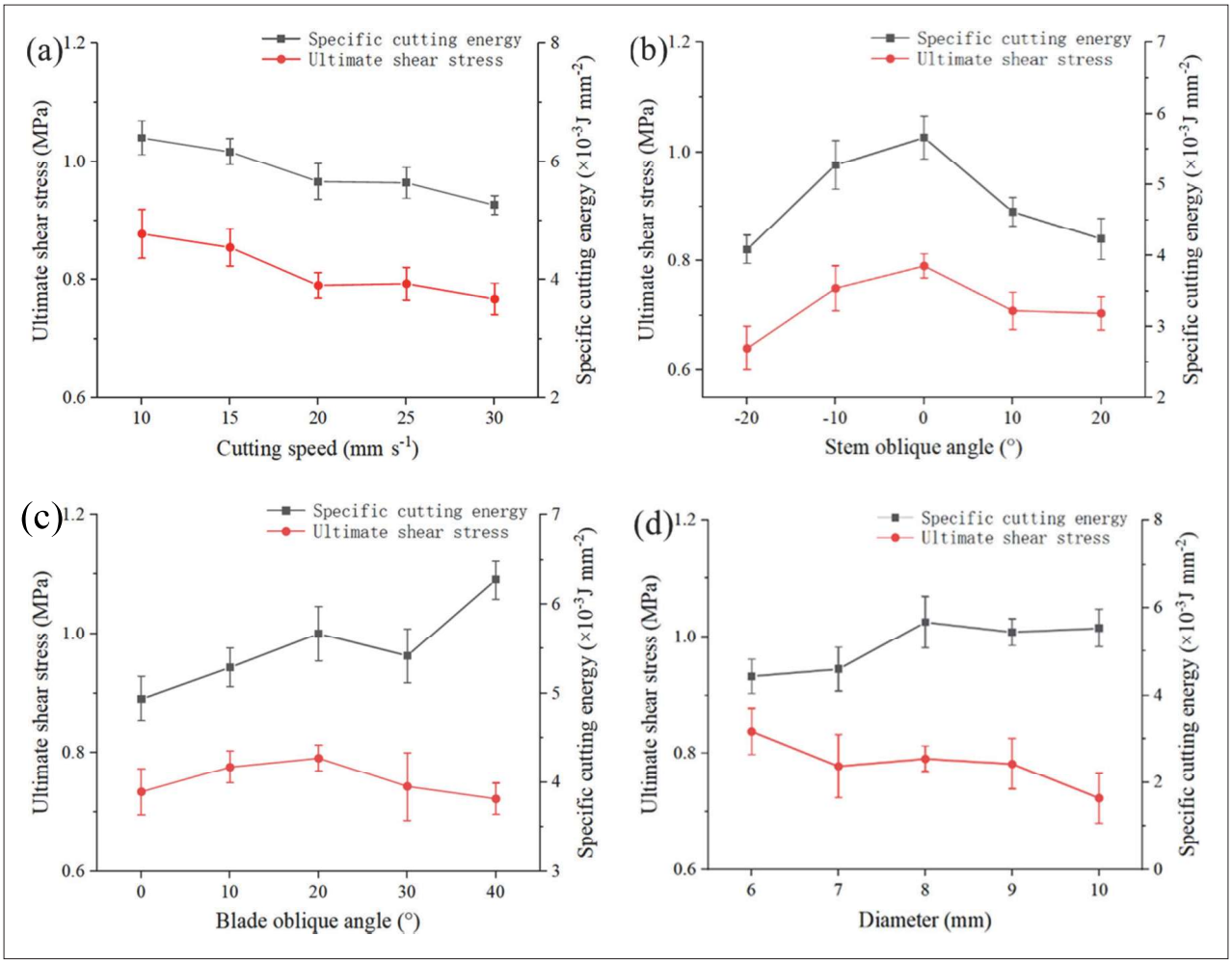


Figure 3. Effects of cutting parameters on cutting: a) cutting speed; b) stem oblique angle; c) blade oblique angle; d) diameter.

Table 4 shows the fit statistics of the two regression models. The coefficients of determination and adjusted coefficients of determination for both models are above 80%, and the differences between the adjusted R^2 and predicted R^2 are all less than 0.2. This indicates that the two regression models are accurate, fit the experimental data, and can be used for further prediction.

Figure 4 shows the effects of interactive items on cutting in Design Expert 11.

By removing the factors that are not significant in variance analysis, the simplified ultimate shear stress response Equation (5) and specific shear energy response Equation (6) can be obtained.

$$\tau = 0.3576 + 0.0078v - 0.0025\alpha + 0.0104\beta + 0.1053D - 0.0004v^2 - 0.0005\alpha^2 - 0.0002\beta^2 - 0.0081D^2 \quad (5)$$

$$E_{pur} = -8.2568 + 0.0445v - 0.0799\alpha - 0.0294\beta + 3.1975D - 0.0049\alpha^2 - 0.1861D^2 \quad (6)$$

With the support of the optimization function in Design Expert 11, the optimal cutting parameters were obtained, which minimize both the ultimate shear stress and specific cutting energy. When the cutting speed is 30 mm s^{-1}, the stem oblique angle is 20°, the blade oblique angle is 0°, and the diameter is 6 mm (Figure 5). According to the calculations based on the above equations, the ultimate shear stress achieves a minimum value of 0.3218 MPa and a specific cutting energy of 2.0056 × 10^{-3} J mm^{-2}. In this case, the peak force is 37.988 N, and the energy consumption is 0.2368 J. Compared to ordinary angle cutting, where both α and β are 0°, the ultimate shear stress and specific cutting energy are reduced by 43.72% and 63.59%, respectively. When the diameter of the cut stem is changed to 10 mm, the optimized cutting still results in a reduction of 52.68% and 55.22% in ultimate shear stress and specific cutting energy, compared to ordinary angle cutting.

In this chapter, with the support of Design Expert 11, the response equations of the ultimate shear stress and specific cutting energy are obtained, and the optimal shear parameters are also obtained. Because there is no in-depth study on weeds, the measurement of these parameters can provide a basis for the design of mowers.

Discussion

Force–displacement curve

Figure 6 illustrates the force-displacement curve from the cutting experiment. This curve can be divided into five distinct stages that explain the detailed cutting process (Igathinathane et al., 2010).

Initially (I), the upper skin of the stem is compressed by the blade without causing any damage. As the compression begins, the upper skin undergoes elastic deformation. However, once the deformation surpasses the biological yield point, the stem skin starts to fail.

Following (II) this, the stem skin at the initial contact

Table 2. Text design and results.

Std. order	Run order	v	α	β	D	τ	E_{pur}
1	30	15	−10	10	7	0.7906	4.9299
2	14	25	−10	10	7	0.7278	4.5996
3	2	15	10	10	7	0.7601	4.3213
4	29	25	10	10	7	0.7017	3.7727
5	18	15	−10	30	7	0.7633	5.0442
6	11	25	−10	30	7	0.7269	4.5852
7	27	15	10	30	7	0.7299	4.4287
8	28	25	10	30	7	0.7064	3.8124
9	25	15	−10	10	9	0.7323	5.496
10	8	25	−10	10	9	0.6881	4.9127
11	15	15	10	10	9	0.7031	4.9192
12	3	25	10	10	9	0.6727	4.3555
13	4	15	−10	30	9	0.699	5.6891
14	9	25	−10	30	9	0.6548	5.1625
15	5	15	10	30	9	0.6729	5.4203
16	19	25	10	30	9	0.6329	4.9011
17	17	10	0	20	8	0.795	6.1185
18	7	30	0	20	8	0.7554	4.9739
19	10	20	−20	20	8	0.6031	3.9846
20	16	20	20	20	8	0.6143	3.5297
21	21	20	0	0	8	0.7338	4.9393
22	6	20	0	40	8	0.7221	6.2714
23	12	20	0	20	6	0.837	4.4315
24	13	20	0	20	10	0.723	5.5313
25	20	20	0	20	8	0.7906	5.6677
26	23	20	0	20	8	0.7752	5.4542
27	22	20	0	20	8	0.816	5.597
28	1	20	0	20	8	0.8059	5.8812
29	26	20	0	20	8	0.8278	5.588
30	24	20	0	20	8	0.8065	5.365

Table 3. Variance analysis of responses.

Source	Ultimate shear stress					Specific cutting energy				
	SS	df	MS	F value	P value	SS	df	MS	F value	P value
Model	0.1069	14	0.0076	21.46	< 0.0001	13.49	14	0.9633	16.99	< 0.0001
v	0.0073	1	0.0073	20.57	0.0004	1.73	1	1.73	30.44	< 0.0001
α	0.0014	1	0.0014	3.82	0.0694	1.21	1	1.21	21.41	0.0003
β	0.0019	1	0.0019	5.35	0.0353	0.8070	1	0.8070	14.23	0.0018
D	0.0192	1	0.0192	53.98	< 0.0001	2.38	1	2.38	42.03	< 0.0001
$v \cdot \alpha$	0.0001	1	0.0001	0.2189	0.6466	0.0076	1	0.0076	0.1340	0.7195
$v \cdot \beta$	0.0002	1	0.0002	0.4696	0.5036	0.0006	1	0.0006	0.0100	0.9217
$v \cdot D$	0.0000	1	0.0000	0.0874	0.7716	0.0036	1	0.0036	0.0628	0.8056
$\alpha \cdot \beta$	$3.062E^{-8}$	1	$3.062E^{-8}$	0.0001	0.9927	0.0265	1	0.0265	0.4672	0.5047
$\alpha \cdot D$	0.0000	1	0.0000	0.0563	0.8157	0.0840	1	0.0840	1.48	0.2422
$\beta \cdot D$	0.0004	1	0.0004	1.21	0.2892	0.0965	1	0.0965	1.70	0.2117
v^2	0.0023	1	0.0023	6.60	0.0214	0.0554	1	0.0554	0.9768	0.3387
α^2	0.0710	1	0.0710	199.55	< 0.0001	6.64	1	6.64	117.20	< 0.0001
β^2	0.0122	1	0.0122	34.21	< 0.0001	0.0249	1	0.0249	0.4397	0.5173
D^2	0.0018	1	0.0018	5.00	0.0410	0.9503	1	0.9503	16.76	0.0010
Residual	0.0053	15	0.0004			0.8504	15	0.0567		
Lack of fit	0.0036	10	0.0004	1.04	0.5138	0.6905	10	0.0690	2.16	0.2047
Pure error	0.0017	5	0.0003			0.1599	5	0.0320		

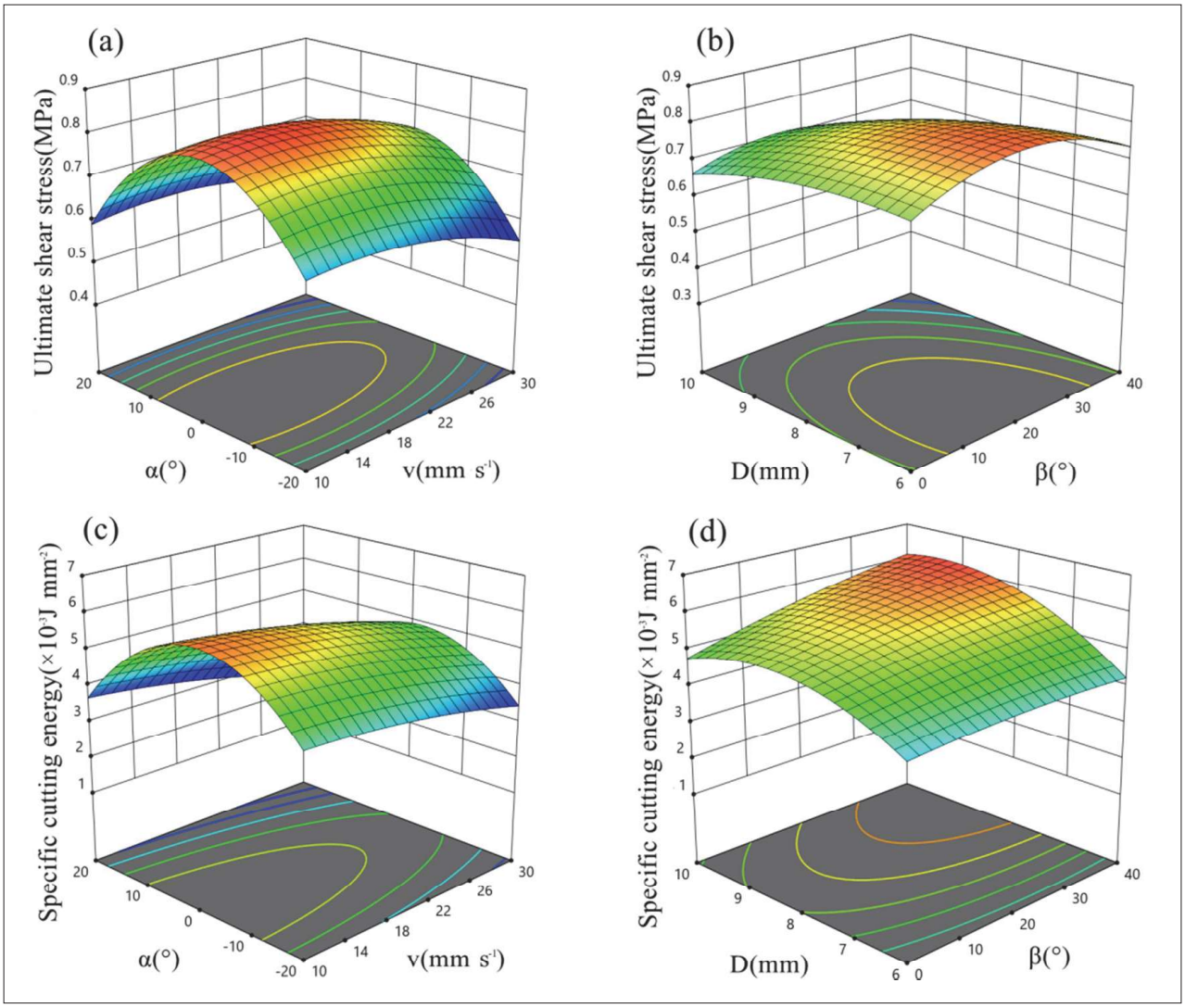


Figure 4. Effects of interactive items on cutting of Canadian goldenrod stem.

point has failed, allowing the blade to cut through the upper skin fibers. As the cutting range of the blade increases, the cutting force rises significantly, resulting in a notable peak on the curve.

After cutting through the upper skin (III), the blade transitions to cutting the skin on both sides and the soft pith. At this stage, the area being cut decreases, leading to a reduction in the cutting force.

As the blade begins to cut the lower skin (IV), the area of the blade's engagement recovers, producing a second peak on the curve.

Eventually (V), the cutting process is completed, but some residual force remains due to the friction between the blade and the sample.

Notably, when cutting the lower skin (IV), the cutting force experiences a substantial increase, significantly surpassing that observed with corn straw. This behavior is reminiscent of the force-displacement curve of sunflower stems (İnce et al., 2005), indicating that, unlike sisal leaves, Canadian goldenrod stems possess tough skin and a soft pith.

Cutting speed

As shown in Figure 3a, when the cutting speed vvv increases, both the ultimate shear stress and specific cutting energy of the Canadian goldenrod stem decrease accordingly. When the cutting speed vvv reaches the maximum value of 30 mm s^{-1}, both the ultimate shear stress and specific cutting energy also reach their minimum values. At low cutting speeds, the process of fiber transitioning from elastic deformation to failure lasts for a long time, prolonging (I) in the cutting process and consuming more energy in extruding the straw fibers. Conversely, at high cutting speeds, the process from elastic deformation to failure is accelerated, resulting in less deformation and lower energy consumption. In summary, increasing the cutting speed will reduce the cutting force, ultimate shear stress, and specific cutting energy (Song et al., 2022).

Table 4. Summary of the regression analysis.

Function	R^2	Adjusted R^2	Predicted R^2
τ	0.9524	0.9080	0.7926
E_{pur}	0.9407	0.8853	0.7065

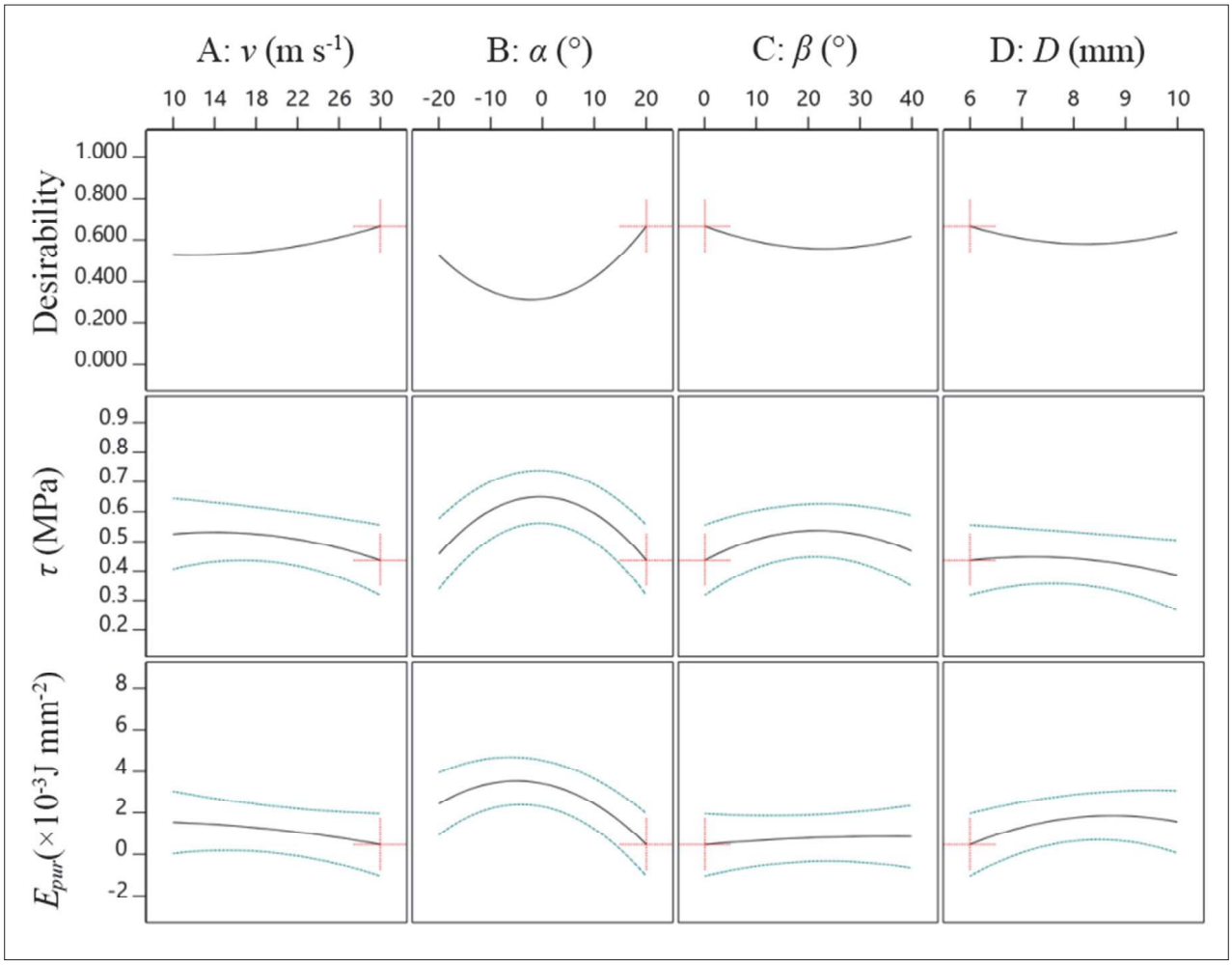


Figure 5. Multi-objective optimisation graph.

When cutting sisal leaves at higher speeds, the deformation of the leaves gradually shifts from plastic deformation to brittle deformation with increasing cutting speed, causing the peak cutting force and cutting energy to gradually decrease until the cutting speed reaches a critical value. The peak cutting force is minimized at a speed of 5 m s^{-1}, while the cutting energy reaches its minimum at 3 m s^{-1} (Song et al., 2022). Yiljep and Mohammed (2005) indicated that the critical value for sorghum cutting speed is 2.9 m s^{-1}, at which the minimum energy is required. When the speed exceeds the corresponding critical value, both the ultimate shear stress and specific cutting energy will increase, which is considered a dissipation of excessive kinetic energy (Taghijarah et al., 2011; Yunfeng et al., 2016; Chandio et al., 2021). Therefore, when the speed is significantly below the critical value, increasing the speed will only reduce the cutting force and energy.

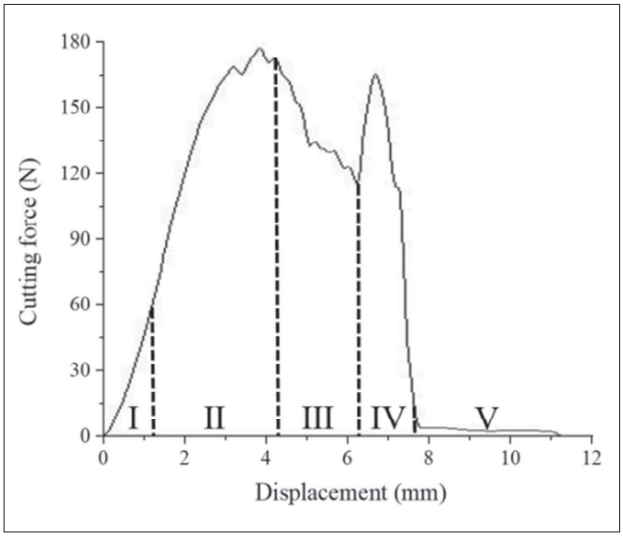


Figure 6. Force-displacement curve.

Stem oblique angle

As shown in Figure 3b, when the stem oblique angle α\alphaα increased from -20° to 20°, both the ultimate shear stress and specific cutting energy of the Canadian goldenrod stem increased before decreasing. Both the ultimate shear stress and specific cutting energy reached their maximum value when α\alphaα was 0°. As the absolute value of α\alphaα decreased, the ultimate shear stress and specific cutting energy increased. This indicates that the stem fibers of Canadian goldenrod have poor cutting resistance in the oblique direction, and their cohesion is easily destroyed. The key to this phenomenon is the structure of the fibers. Igathinathane et al. (2010) found that the smaller the angle between the fiber and the blade, the smaller the peak force, ultimate shear stress, and cutting energy. When the angle is 0°, with the fibers parallel to the stem, the peak force, ultimate shear stress, and cutting energy reach their minimum values. Ghahraei et al. (2011) found that the angle between the fiber and blade helps save cutting energy.

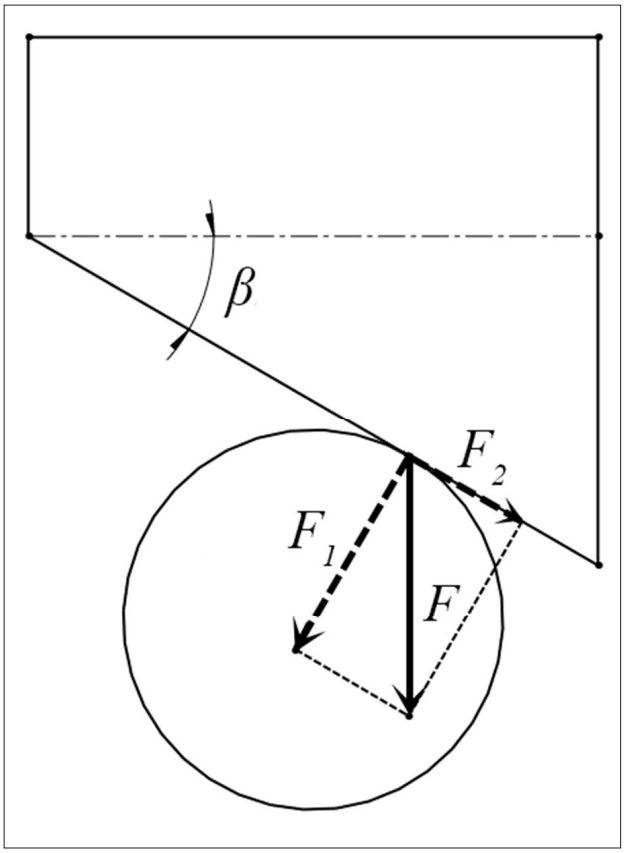


Figure 7. Schematic diagram of force distribution when cutting with blade oblique angle.

Blade oblique angle

As shown in Figure 3c, as the blade oblique angle β\betaβ increased, the ultimate shear stress rose when the blade oblique angle was less than 20° and then dropped, while the specific cutting energy consistently increased with the angle. Although the oblique blade can effectively reduce the blade wedge angle during cutting (Moiceanu et al., 2017), the blade oblique angle also changes the direction of the cutting force on the stem. As shown in Figure 7, when cutting with a blade oblique angle β\betaβ, only a portion of the cutting force is used to cut fibers longitudinally, producing elastic or plastic deformation (F1), while the remainder is used to cut the fibers transversely (F2). Since the skin has strong transverse cutting resistance, F2 provides minimal benefit, reaching its threshold at 20°. The increase in blade oblique angle β\betaβ becomes unfavorable for reducing ultimate shear stress when the blade angle is less than 20°. In conclusion, as the blade oblique angle β\betaβ increases, the reduction in blade wedge angle will help to decrease the stress, while the change in direction of the force will contribute to increasing the stress. When the blade oblique angle β\betaβ is less than 20°, the effect of the change in the direction of the force is greater than that of the reduction in the blade wedge angle, resulting in an increase in ultimate shear stress. Conversely, when the blade oblique angle β\betaβ exceeds 20°, the situation reverses, leading to a decrease in ultimate shear stress. Although the ultimate shear stress varies with the increasing blade oblique angle, the change is not substantial. The increase in the blade oblique angle β\betaβ will effectively extend the cutting distance of the blade, thereby significantly increasing the specific cutting energy consumed during cutting.

Diameter

As shown in Figure 3d, with increasing diameter DDD, the ultimate shear stress decreases, while the specific cutting energy increases. Although the ultimate shear stress and specific cutting energy calculations have removed the influence of diameter DDD on the numerical value, they represent values per unit area and still exhibit different performances under varying diameters due to structural heterogeneity (İnce et al., 2005). As DDD decreases, the pith also decreases correspondingly. In the upper part of the stem, the proportion of skin becomes larger, resulting in an increase in ultimate shear stress. With increasing diameter, the proportion of mature fibers in the stem skin fibers is larger (İnce et al., 2005), leading to an increase in the shear area and friction, which requires more energy to cut.

Effects of interactive items on cutting of Canadian goldenrod stems

In Figures 4a and c, the increase in cutting speed and the absolute value of the stem oblique angle can reduce the ultimate shear stress and specific cutting energy. The increase in cutting speed helps accelerate the process of fiber failure and reduces energy loss. Additionally, the increase in the absolute value of the stem oblique angle allows the blade to cut in a manner that offers low cutting resistance. In Figure 4b, a larger diameter and blade oblique angle help to reduce the ultimate shear stress; however, the ultimate shear stress will rise first and then fall due to the interplay between the reduction of the blade wedge angle and the change in force direction. The lower skin with a larger diameter accounts for less surface area, while the larger blade oblique angle can further reduce the blade wedge angle. In Figure 4d, the larger diameter and blade oblique angle contribute to an increase in specific cutting energy. When cutting stems with a larger diameter, the cutting area is larger and the resistance is greater, while a larger blade oblique angle leads to an increased cutting area, which ultimately results in an increase in specific cutting energy.

Practical implications

This study presents the mechanical properties of a weed with thick stems. The cutting force and power consumption may vary in different directions, indicating that a lawn mower or harvester could benefit from a tilting blade group. Different blade angles result in varying cutting forces and power consumption, highlighting the potential for optimizing the curvature of the cutting edge. In the optimization process for the power consumption and cutting torque of lawn mowers, the mechanical properties of the cutting object are fundamental.

Conclusions

Under the condition of quasi-static cutting, using a combination of single-factor cutting experiments and response surface cutting experiments, the force-displacement curve representing the cutting process is obtained, which can be divided into five parts. This paper presents the specific effects of different cutting factors – cutting speed, blade angle, stem angle, and stem diameter – on the cutting process, ultimate shear stress, and specific cutting energy. All these factors significantly affect the force-displacement curve during cutting, revealing some of the physical characteristics of Canadian goldenrod stems. When cutting close to the ground, the optimized cutting method reduces the ultimate shear stress and specific cutting energy by 52.68% and 55.22%, respectively, compared to ordinary cutting.

This research can provide a reference for harvesting machinery in Canada, as well as guidance for manual harvesting and weeding. Based on the optimal value of stem diameter, raising the cutting position when cutting a yellow flower can help reduce the ultimate shear stress. Furthermore, based on the optimal value of the stem oblique angle, the cutting direction can be angled with respect to the stem, effectively reducing the peak cutting force and energy consumption under safe conditions.

Acknowledgment

The authors declare that they have no known competing financial interests or personal relationships that could have appeared to influence the work reported in this paper.

Author contribution statement

Z.L.: Focus on writing papers and conducting experiments.
W.J., M.O., X.D., T.Z.: Emphasis on revising the paper and proposing experimental plans.
G.W., H.C., C.W.: Focus on revising the paper and conducting experiments.

Funding

The article was funded by A Project Funded by the Priority Academic Program Development of Jiangsu Higher Education Institutions (PAPD-2023-87), Jiangsu Province agricultural machinery R&D, manufacturing, promotion and application integration pilot project (JSYTH05) and Jiangsu Province and Education Ministry Co-sponsored Synergistic Innovation Center of Modern Agricultural Equipment (XTCX1003).

Competing interests

The authors declare none.

References

Abhilasha, D., Quintana, N., Vivanco, J., and Joshi, J. (2008). Do allelopathic compounds in invasive *Solidago canadensis* S.L. restrain the native European flora? J. Ecology *96*(5), 993–1001. https://doi.org/10.1111/j.1365-2745.2008.01413.x.

Apati, P., Szentmihalyi, K., Kristo, S.T., et al. (2003). Herbal remedies of *Solidago* – Correlation of phytochemical characteristics and antioxidative properties. J. Pharmaceut. Biomed. Anal. *32*(4–5), 1045–1053. https://doi.org/10.1016/S0731-7085(03)00207-3.

ASABE Standards. (2008). S358. 2: Moisture measurement-forages (St. Joseph, U.S.A.: ASABE).

Aydın, İ., and Arslan, S. (2018). Mechanical properties of cotton shoots for topping. Industr. Crops Prod. *112*, 396–401. https://doi.org/10.1016/j.indcrop.2017.12.036.

Chandio, F.A., Li, Y., Ma, Z., et al. (2021). Influences of moisture content and compressive loading speed on the mechanical properties of maize grain orientations. Intl. J. Agric. Biol. Engin. *14*(5), 41–49.

Dange, A.R., Thakare, S.K., and Rao, I.B. (2011). Cutting energy and force as required for Pigeon pea stems. J. Agric. Technol. *7*, 1485–1493.

Dong, M., Lu, J.Z., Zhang, W.J., Chen, J.K., and Li, B. (2006). Canada goldenrod (*Solidago canadensis*): An invasive alien weed rapidly spreading in China. J. System. Evol. *44*(1), 72–85. https://doi.org/10.1360/aps050068.

Du, D., Wang, J., and Qiu, S. (2015). Analysis and test of splitting failure in the cutting process of cabbage root. Intl. J. Agric. Biol. Engin. *8*(4), 27–34.

Engmann, F.N., Ma, Y., Zhang, H., et al. (2014). The application of response surface methodology in studying the effect of heat and high hydrostatic pressure on anthocyanins, polyphenol oxidase, and peroxidase of mulberry (*Morus nigra*) juice. J. Sci. Food Agric. *94*(11), 2345–2356.

Ghahraei, O., Ahmad, D., Khalina, A., Suryanto, H., and Othman, J. (2011). Cutting tests of kenaf stems. Transactions ASABE *54*(1), 51–56. https://doi.org/10.13031/2013.36252.

Ghahraei, O., Khoshtaghaza, M.H., and Ahmad, D.B. (2008). Design and development of special cutting system for sweet Sorghum harvester. J. Central Eur. Agric. *9*, 469–474.

Hu, J., Xu, L., Yu, Y., et al. (2023). Design and experiment of bionic straw-cutting blades based on locusta migratoria manilensis. Agriculture *13*(12), 2231. https://doi.org/10.3390/agriculture13122231.

Hu, Z., Li, J., Shi, K., Ren, G., Dai, Z., Sun, J., and Du, D. (2021). Effects of Canada Goldenrod invasion on soil extracellular enzyme activities and ecoenzymatic stoichiometry. Sustainability *13*, 3768. https://doi.org/10.3390/su13073768.

Igathinathane, C., Womac, A.R., and Sokhansanj, S. (2010). Corn stalk orientation effect on mechanical cutting. Biosyst. Engin. *107*(2), 97–106. https://doi.org/10.1016/j.biosystemseng.2010.07.005.

İnce, A., Uğurluay, S., Güzel, E., and Özcan, M.T. (2005). Bending and shearing characteristics of sunflower stalk residue. Biosyst. Engin. *92*(2), 175–181. https://doi.org/10.1016/j.biosystemseng.2005.07.003.

Johnson, P.C., Clementson, C.L., Mathanker, S.K., Grift, T.E., and Hansen, A.C. (2012). Cutting energy characteristics of *Miscanthus* × *giganteus* stems with varying oblique angle and cutting speed. Biosyst. Engin. *112*(1), 42–48. https://doi.org/10.1016/j.biosystemseng.2012.02.003.

Leitner, P., Fitz-Binder, C., Mahmud-Ali, A., et al. (2012). Production of a concentrated natural dye from Canadian Goldenrod (*Solidago canadensis*) extracts. Dyes and Pigments *93*(1–3), 1416–1421. https://doi.org/10.1016/j.dyepig.2011.10.008.

Mathanker, S.K., Grift, T.E., and Hansen, A.C. (2015). Effect of blade oblique angle and cutting speed on cutting energy for energycane stems. Biosyst. Engin. *133*, 64–70. https://doi.org/10.1016/j.biosystemseng.2015.03.003.

Maughan, J.D., Mathanker, S.K., Fehrenbacher, B.M., and Hansen, A.C. (2014). Impact of cutting speed and blade configuration on energy requirement for *Miscanthus* harvesting. Appl. Engin. in Agric. *30*(2), 137–142. https://doi.org/10.13031/aea.30.10161.

McRandal, D.M., and McNulty, P.B. (1978). Impact cutting behaviour of forage crops. I. Mathematical models and laboratory tests. J. Agric. Engin. Res. *23*(3), 313–328. https://doi.org/10.1016/0021-8634(78)90104-x.

Moiceanu, G., Voicu, P., Paraschiv, G., and Voicu, G. (2017). Behaviour of *Miscanthus* at cutting shear with straight knives with different edge angles. Environm. Engin. Manag. J. *16*, 1203–1209. https://doi.org/10.30638/eemj.2017.126.

Rabbani, H., Sohraby, N., Gholami, R., Jaliliantabar, F., and Waismorady, A. (2015). Determination of mass density module, crush resistance coefficient and cutting efficiency of rose (*Rosa damascene* Mill.). Sci. Hortic. *190*, 144–148. https://doi.org/10.1016/j.scienta.2015.02.009.

Ruyi, Y., Guodong, Y., Tang, J., and Xin, C. (2008). Effects of metal lead on growth and mycorrhizae of an invasive plant species (*Solidago canadensis* L.). J. Environm. Sci. *20*(6), 739–744. https://doi.org/10.1016/s1001-0742(08)62121-x.

Song, S., Zhou, H., Jia, Z., Xu, L., Zhang, C., Shi, M., and Hu, G. (2022a). Effects of cutting parameters on the ultimate shear stress and

specific cutting energy of sisal leaves. Biosyst. Engin. *218*, 189–199. https://doi.org/10.1016/j.biosystemseng.2022.03.011.

Song, S., Zhou, H., Xu, L., Jia, Z., and Hu, G. (2022b). Cutting mechanical properties of sisal leaves under rotary impact cutting. Industr. Crops Prod. *182*, 114856. https://doi.org/10.1016/j.indcrop.2022.114856.

Suleymanova, F.S., Nesterova, O.V., Avertseva, I.N., et al. (2020). Antioxidant and antibacterial activity of the Canadian Goldenrod herb (*Solidago canadensis* L.). Moscow Univ. Chem. Bull. *75*, 261–263. https://doi.org/10.3103/S0027131420040070.

Taghijarah, H., Ahmadi, H., Ghahderijani, M., and Tavakoli, M. (2011). Cutting forces and energy during an impact cut of sugarcane stalks. Austral. J. Crop Sci. *5*, 630–634.

Tang, Z., Liang, Y., Wang, M., et al. (2022). Effect of mechanical properties of rice stem and its fiber on the strength of straw rope. Industr. Crops Prod. *180*, 114729.

Tu, J., Qiao, Z., Wang, Y., et al. (2023). Biomass-based porous carbon for high-performance supercapacitor electrode materials prepared from Canada goldenrod. J. Energy Storage *73*, 109268. https://doi.org/10.1016/j.est.2023.109268.

Vu, V.D., Ngo, Q.H., Nguyen, T.T., Nguyen, H.C., Nguyen, Q.T., and Nguyen, V.D. (2020). Multi-objective optimisation of cutting force and cutting power in chopping agricultural residues. Biosyst. Engin. *191*(6), 107–115. https://doi.org/10.1016/j.biosystemseng.2020.01.007.

Wang, C., Wu, B., Jiang, K., Zhou, J., Liu, J., and Lv, Y. (2019). Canada goldenrod invasion cause significant shifts in the taxonomic diversity and community stability of plant communities in heterogeneous landscapes in urban ecosystems in East China. Ecol. Engin. *127*, 504–509. https://doi.org/10.1016/j.ecoleng.2018.10.002.

Wang, W., Wang, S., Zhang, J., et al. (2022). Experiment and research on cutting mechanical properties of little cabbage. Appl. Sci. *12*(4), 2060. https://doi.org/10.3390/app12042060.

Wang, Y., Yang, Y., Zhao, H., Liu, B., Ma, J., He, Y., and Xu, H. (2020). Effects of cutting parameters on cutting of citrus fruit stems. Biosyst. Engin. *193*, 1–11. https://doi.org/10.1016/j.biosystemseng.2020.02.009.

Wu, K., and Song, Y. (2022). Research progress analysis of crop stalk cutting theory and method. Transact. Chinese Soc. Agric. Machinery *53*, 1–20.

Yiljep, Y.D., and Mohammed, U.S. (2005). Effect of knife velocity on cutting energy and efficiency during impact cutting of sorghum stalk (Belgium: Intl. Comm. Agric. Engin.).

Yunfeng, X., Xiliang, Z., Xiaojia, S., et al. (2016). Tensile mechanical properties of greenhouse cucumber cane. Intl. J. Agric. Biol. Engin. *9*(5), 1–8.

Zhang, F., and Wan, F.H. (2017). Canada Goldenrod *Solidago canadensis* L. In Biological Invasions and Its Management in China (Singapore: Springer), p. 143–151.

Zhao, S.Y., Sun, S.G., Dai, C., Gituru, R.W., Chen, J.M., and Wang, Q.F. (2015). Genetic variation and structure in native and invasive *Solidago canadensis* populations. Weed Res. *55*(2), 163–172. https://doi.org/10.1111/wre.12130.

Zhao, Y., Tang, Z., and Chen, S. (2022). Loading model and mechanical properties of mature broccoli (*Brassica oleracea* L. var. Italica Plenck) stems at harvest. Agriculture *12*(10), 1519.

Received: Jun. 11, 2024
Accepted: Oct. 8, 2024

Addresses of authors:
Ziyu Li[1], Guanqun Wang[1], Weidong Jia[1,*], Mingxiong Ou[1], Xiang Dong[1], Tie Zhang[2], Hong Chen[1] and Chenyang Wang[1]
[1] School of Agricultural Engineering, Jiangsu University, Zhenjiang 212013, China
[2] Chinese Academy of Agricultural Mechanization Sciences Group Co., Ltd., Beijing 100083, China
* Corresponding author; E-mail: jwd_ujs@163.com